Case report

MYC/*BCL2* double- and *MYC*/*BCL2*/*BCL6* triple-hit follicular lymphomas associated with t(8;14;18) (q24;q32;q21)

Kayo Takeoka,[1)] Fumiyo Maekawa,[1)] Miho Nakagawa,[1)] Chiyuki Kishimori,[1)]

Katsuhiro Fukutsuka,[1)] Masahiko Hayashida,[1)] Shinji Sumiyoshi,[2)] Hitoshi Ohno[1)]

We describe two follicular lymphoma (FL) patients with *MYC*/*BCL2* double- and *MYC*/*BCL2*/*BCL6* triple-hit translocations. The first patient (case 1) was a man in his 30s who presented with stage IV disease with leukemic manifestation. The second patient (case 2) was a man in his 60s who presented with relapsed FL, but his disease was in a limited stage. Histopathology of the lymph node biopsies revealed grade 3A FL in both cases. MYC positivity and the Ki-67–labeling index were 60–70 and 20% in case 1 and 30 and 50% in case 2, respectively. G-banding revealed t(8;14;18)(q24;q32;q21) in both cases and fluorescence *in situ* hybridization using *MYC*, *IGH*, and *BCL2* break-apart probes confirmed t(8;14;18)(+5′BCL2,−3′MYC;+3′MYC,−5′IGH;+5′IGH,−5′BCL2). In case 2, additional materials of der(8)t(8;14;18) were duplicated and translocated to chromosome Y, and t(3;16)(q27;p13)/*BCL6*::*CIITA* was identified. We obtained *BCL2*-major breakpoint region::*IGHJ5*::*IGHG1* and *MYC* exon 2::*IGHA2* fusion sequences by long-distance polymerase chain reaction in case 1, and proposed that t(8;14;18) was generated by two-step translocations and that *BCL2*::*IGH* and *MYC*::*IGH* involved the same *IGH* allele. Both patients responded to the standard chemotherapy for FL. We suggest that the presence of t(8;14;18) in FL does not immediately indicate high-grade transformation and aggressive clinical behavior requiring intensive chemotherapy.

Keywords: follicular lymphoma, double-/triple-hit translocation, t(8;14;18)(q24;q32;q21), G-banding, fluorescence *in situ* hybridization

INTRODUCTION

High-grade B-cell lymphoma (HGBL/HGBCL) with *MYC* and *BCL2* and/or *BCL6* rearrangements, proposed by the WHO Classification of Tumours of Haematopoietic and Lymphoid Tissues in 2017,[1] has been renamed as diffuse large B-cell lymphoma (DLBCL)/HGBL with *MYC* and *BCL2* rearrangements in the upcoming 5th edition of the WHO Classification of Haematolymphoid Tumours focusing on lymphoid neoplasms,[2] and HGBCL with *MYC* and *BCL2* rearrangements in the International Consensus Classification of Mature Lymphoid Neoplasms.[3] This new entity is defined by the presence of dual *MYC* and *BCL2* rearrangements, but not dual *MYC* and *BCL6* rearrangements, and is associated with an exclusive germinal center (GC) gene expression profile and a close pathogenetic relationship to follicular lymphoma (FL) and molecular GC-like DLBCL subsets.[2] At present, however, the names of double-hit (DH) and triple-hit

(TH) lymphomas are preferably used in clinical practice.[1,4,5] Most patients with DH/TH lymphoma present with advanced disease involving extranodal sites and high international prognostic index scores.[1] The response to conventional chemotherapy is poor and a more intensive treatment approach is required.[4,5]

In contrast, FL is the most common subtype of low-grade B-cell lymphomas.[6] The majority of cases of FL are characterized by t(14;18)(q32;q21) that fuses *BCL2* on 18q21 to *IGH* on 14q32.[7] 3q27/*BCL6* rearrangements sometimes coexist with t(14;18),[8,9] but the association of 8q24/*MYC* abnormalities is uncommon at diagnosis.[7,10] However, three independent groups consecutively published large case series of FL with DH/TH rearrangements (DH/TH-FL), in which the DH/TH status was determined by fluorescence *in situ* hybridization (FISH) applied to tissue sections.[11-13] According to these studies, DH/TH-FL shares general clinical and immunohistochemical characteristics of FL, but often

shows grade 3 histopathology.[11-13] MYC positivity and the Ki-67–labeling index were variable among cases and studies. Compared with HGBL with *MYC* and *BCL2* and/or *BCL6* rearrangements, the genomic profile of DH/TH-FL showed fewer copy-number alterations.[12] Patients were treated with variable regimens and most patients achieved a complete response.[11,12,14] However, as the numbers of cases studied were small, the significance of DH/TH in the treatment outcome of FL remains to be determined.

Here, we describe two cases of FL of the grade 3A category carrying *MYC*/*BCL2* DH and *MYC*/*BCL2*/*BCL6* TH translocations. G-banding and FISH applied to the metaphase spreads revealed that both cases had t(8;14;18)(q24;q32;q21), which is a cytogenetic equivalent of concurrent t(8;14)(q24;q32) and t(14;18)(q32;q21), but involves a single *IGH* allele. Their clinical, histopathologic, and cytogenetic features and DNA studies are presented.

MATERIALS AND METHODS

Case presentation

Case 1: A man in his 30s presented with cervical lymphadenopathy. He had noticed night sweating. His father had developed Hodgkin lymphoma at the age of 63 followed by DLBCL at 66 and died of progression. ^{18}F-fluorodeoxyglucose-positron emission tomography combined with computed tomography (^{18}F-FDG-PET/CT) revealed accumulation of the tracer within not only multiple cervical lymph nodes, but also those in the subclavicular, axillary, mediastinal, paraaortic, mesenteric iliac, and inguinal regions and spleen. His hemoglobin level was 14.4 g/dL, white cell count was 7.25×10^3/μL, and platelet count was 236×10^3/μL. The white cell differential included 31.5% atypical lymphocytes with nuclear clefts and basophilic cytoplasm. The level of lactate dehydrogenase was 266 U/L (reference range, 124 to 222 U/L), albumin was 4.2 g/dL, uric acid was 5.5 mg/dL, C-reactive protein was 0.09 mg/dL, soluble interleukin-2 receptor (sIL-2R) was 1,728 U/mL (reference range, 122 to 496 U/mL), and β2 microglobulin was 1.42 μg/mL (reference range, 0.8 to 1.9 μg/mL). The bone marrow (BM) included 2.9% atypical lymphocytes. He underwent biopsy of the cervical LN, demonstrating FL. His ECOG performance status (PS) was 1. He was treated with 6 cycles of cyclophosphamide, doxorubicin, vincristine, and prednisolone (CHOP) in combination with obinututumab, leading to a complete metabolic response based on ^{18}F-FDG-PET/CT after completion of the treatment. He is currently receiving maintenance treatment of obinutuzumab 1 year and 6 months after initial presentation.

Case 2: A man in his 60s presented with submental lymphadenopathy. Eleven years earlier, he had received 6 cycles of CHOP in combination with rituximab (R) for the treatment of stage III FL and maintained a complete response until this presentation. ^{18}F-FDG-PET/CT confirmed accumulation of the tracer in the submental and left submandibular LNs, and FDG-avid LNs were found in the mediastinum. His blood cell count and blood chemistry were unremarkable.

sIL-2R was 492 U/mL and β2 microglobulin was 2.21 μg/mL. His ECOG PS was 0. Biopsy of the submental LN demonstrated recurrence of FL. He was treated with 6 cycles of bendamustine and obinututumab, leading to resolution of the lymphoma lesions. He is currently receiving maintenance treatment of obinutuzumab 2 years after relapse.

Histopathology

Pathological specimens were fixed in 10% neutral buffered formalin, embedded in paraffin, and then subjected to histopathological examination. For immunohistochemistry (IHC), paraffin-embedded sections were deparaffinized and rehydrated, and heat-induced epitope retrieval was employed according to the antibody to be applied. Sections were incubated with the peroxidase-conjugated secondary antibody (Histofine® Simple Stain MAX PO [MULTI], #424154; Nichirei Biosciences, Tokyo, Japan), and peroxidase was visualized with diaminobenzidine (#347-00904; Nichirei Biosciences). Sections were then counterstained with hematoxylin and cover-slipped.

Flowcytometry

LN biopsies were aseptically minced to prepare a cell suspension, then subjected to flowcytometry (FCM). Fluorescence was captured using a NAVIOS 3L flow cytometer and analyzed by Kaluza Flow Cytometry Analysis Software (Beckman Coulter, Brea, CA, USA). The expression of each antigen in lymphoma cells was graded as negative (−), dim, positive (+), or bright (++) compared with that in reactive B cells.

G-banding and FISH

Cytogenetic preparations were obtained according to the established method and chromosomes were banded by trypsin-Giemsa. FISH probes were: Vysis LSI *MYC*, *IGH*, *BCL2*, and *BCL6* dual-color break-apart (BA) probes, a *BCL2-IGH* dual-color dual-fusion (DF) probe (Abbott Laboratories, Abbott Park, IL, USA), and a *CIITA* BA probe (Empire Genomics, Williamsville, NY, USA). Denaturing of the chromosome/probe, hybridization, and washing conditions were as recommended by the manufacturers. FISH images were photographed using fluorescence microscopes (Nikon Corporation, Tokyo, Japan) equipped with DAPI, tetramethylrhodamine B isothiocyanate (TRITC), and fluorescein isothiocyanate (FITC) fluorescence filters, as well as a DAPI/FITC/TRITC triple band-pass filter. The results of the cytogenetic analysis were described according to the ISCN 2020.[15]

Long-distance polymerase chain reaction (LD-PCR) and direct sequencing

Genomic DNA was isolated from the cell suspension of the biopsies by means of proteinase K and phenol/chloroform. The sequences of the primers for LD-PCR to encompass the t(8;14)(q24;q32)/*MYC*::*IGH* and t(14;18)(q32;q21)/*BCL2*::*IGH* junctions, as well as the PCR parameters, were as described previously.[16] PCR amplification was performed

in a Veriti 96-well thermal cycler (Thermo Fisher Scientific, Waltham, MA, USA). The PCR products were visualized by ethidium bromide (EtBr)-stained agarose gel electrophoresis, purified using a MinElute® PCR Purification Kit (#28004; QIAGEN, Hilden, Germany), subjected to a cycle sequencing reaction (BigDye® Direct Cycle Sequencing Kit, #4458688; Thermo Fisher Scientific), and then sequenced using SeqStudio™ Genetic Analyzer (Thermo Fisher Scientific).

RESULTS

Examination of tumor specimens

The biopsy specimens of both cases were effaced with back-to-back pattern follicles, which were highlighted by the anti-CD21 IHC for follicular dendritic cell network (Figures 1A and B). Tumor cells were medium to large and there were areas where centroblasts were predominant (> 15 per high-power microscopic field), corresponding to the grade 3A category of FL. The cells were positive for CD20 and BCL2 and negative for CD3 and CD5. Case 1 was positive for CD10, but case 2 was negative for the expression. MYC positivity was 60 to 70% in case 1 and 30% in case 2. BCL6 was positive and IRF4/MUM1 was negative in case 2. The Ki-67–labeling indices were 20% in case 1 and 50% in case 2 (Figures 1A and B).

Mononuclear cells were selected using the CD45/side scatter (SSC) and forward scatter (FSC)/SSC gating strategies, and the cells were subjected to multicolor flow cytometry (Figure 2). Lymphoma cells and reactive polyclonal B cells were effectively separated by the expression of HLA-DR/CD19 (case 1) and CD38/CD19 (case 2). When compared with polyclonal B-cell populations, lymphoma cells in both cases showed higher FSC values, in accordance with the cell sizes recognized by the histopathological examination. Lymphoma cells in case 1 were CD19^{dim}, CD20$^+$, CD5$^-$, CD10$^+$, CD38$^+$, and HLA-DR^{++} and expressed the λ light chain (Figure 2A). Similarly, circulating atypical lymphocytes showed the same surface antigen expression. On the other hand, lymphoma cells in case 2 were CD19$^{dim/+}$, CD20$^+$, CD5$^-$, CD10$^-$, CD38$^{+/dim}$, and HLA-DR$^+$ and expressed the λ light chain (Figure 2B). Heavy chains were μδ in case 1 and γ in case 2. DNA indices were 1.00 and 1.11, respectively.

Cytogenetic studies

Metaphase spreads obtained from short-term culture of lymphoma cells were subjected to cytogenetic analyses. G-banding of both cases revealed abnormalities of the long arms of chromosomes 8 [der(8)], 14 [der(14)], and 18 [der(18)] (Figure 3). We performed FISH using the MYC (8q24), IGH (14q32), and BCL2 (18q21) BA probes and found that the telomeric 3′ MYC hybridization signal was translocated to der(14), telomeric 5′ IGH signal to der(18), and telomeric 5′ BCL2 signal to der(8), respectively. We thus determined that the three derivative chromosomes represented t(8;14;18)(q24;q32;q21).ish t(8;14;18)(+5′BCL2,−3′M

YC;+3′MYC,−5′IGH;+5′IGH,−5′BCL2) (Figures 4A and 5A). In case 1, after hybridization with the BCL2-IGH DF probe, der(8) and der(18) were labeled with the BCL2::IGH fusion signal (Figure 4B). Accordingly, interphase nuclei exhibited one red (BCL2), two green (IGH), and two yellow (BCL2::IGH fusion) hybridization signals (Figure 4C).

Additional cytogenetic abnormalities in case 1 were numerical abnormalities: +X, +7, +11, and +12 (Figure 3A). On the other hand, case 2 included add(Y)(q12), der(3), and ider(16)(p10) marker chromosomes (Figure 3B). FISH using the MYC and BCL2 BA probes revealed that the 5′ MYC and 5′ BCL2 signals were colocalized on the add(Y) [add(Y)(q12).ish (+5′MYC,+5′BCL2)] (Figure 5A), suggesting that additional materials of add(Y) were a duplicate of those of der(8). FISH with the BCL6 BA probe revealed that centromeric 3′ BCL6 remained on der(3) and both telomeric ends of ider(16)(p10) were labeled with the telomeric 5′ BCL6 signals (Figure 5B). As CIITA mapped at 16p13.13 was reported to be rearranged with BCL6,[17] we rehybridized the metaphase spread with the CIITA BA probe. As shown in Figure 5B, der(3) was labeled with the telomeric 5′ CIITA probe and both ends of ider(16)(p10) were labeled with the centromeric 3′ CIITA probe, confirming the generation of the BCL6::CIITA fusion gene. Thus, der(3) and ider(16)(p10) are described as der(3)t(3;16)(q27;p13).ish der(3) (−5′BCL6,+5′CIITA) and ider(16)(p10)t(3;16)(q27;p13.13). ish ider(16)(p10)(+5′BCL6×2,−5′CIITA×2), respectively.

Anatomy of t(8;14;18)(q24;q32;q21)

G-banding and FISH suggested that der(8) carried 5′ BCL2::3′ IGH::5′ MYC, der(14) carried 3′ MYC::3′ IGH, and der(18) carried 5′ IGH::3′ BCL2 in the telomere to centromere orientation. In case 2, it is likely that the 5′ BCL2::3′ IGH::5′ MYC triple fusion element was duplicated and translocated to the telomeric end of chromosome Y to create add(Y)(q12). To confirm these fusion sequences on the three derivative chromosomes, we performed LD-PCR to amplify the DNA encompassing the junctions in case 1. Combinations of BCL2-major breakpoint cluster (MBR) and IGH-En and IGHG primers generated 4.6- and 6.5-kb products (Figure 6A, arrows), and nucleotide sequencing revealed the sequences of BCL2-MBR followed by IGHJ5, IGHJ3P, and IGHJ6, as well as those of IGHG1. LD-PCR products 10.0 kb in size generated by the MYC and IGHA primer combination included sequences of MYC exon 2 and IGHA2 (Figure 6B, arrow).

DISCUSSION

Here, we described two cases of grade 3A FL associated with MYC/BCL2 DH (case 1) and MYC/BCL2/BCL6 TH (case 2) translocations. Case 1 had stage IV disease with leukemic manifestation, while case 2 presented with relapsed disease after long-term remission, but the disease was in a limited stage and the tumor burden was small. Case 1 was positive for MYC expression, and the expression in case 2 was below the 40% cut-off in IHC. On the contrary, the
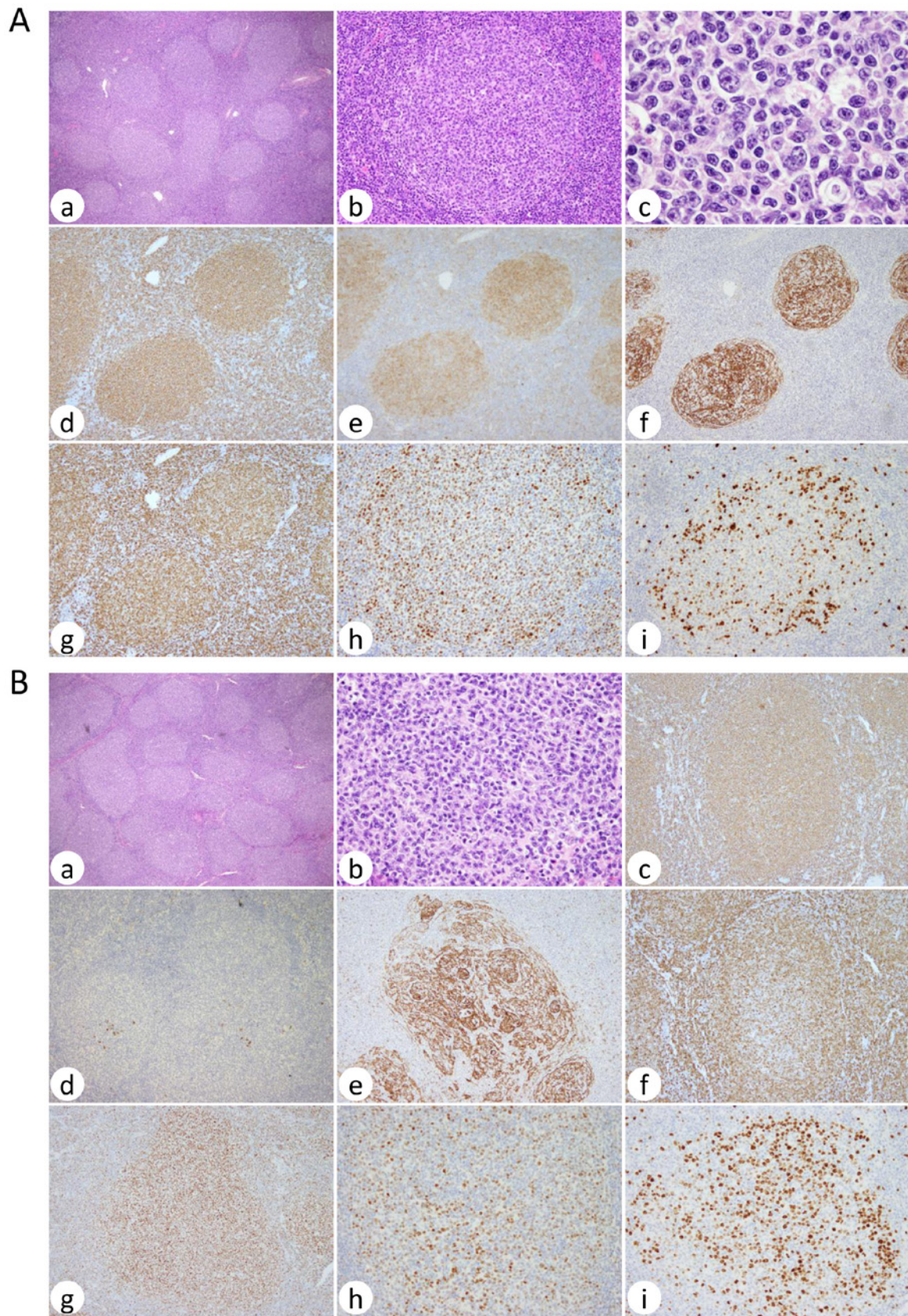
Fig. 1. Histopathology of the LN biopsy. (***A***) Case 1. ***a***, hematoxylin & eosin (H&E) staining (original magnification of objective lens, 4×); ***b***, H&E (20×); ***c***, H&E (100×); ***d***, anti-CD20 immunostaining (10×); ***e***, anti-CD10 (10×); ***f***, anti-CD21 (10×); ***g***, anti-BCL2 (10×); ***h***, anti-MYC (20×); and ***i***, anti-Ki-67 (20×). (***B***) Case 2. ***a***, H&E staining (4×); ***b***, H&E (40×); ***c***, anti-CD20 immunostaining (10×); ***d***, anti-CD10 (10×); ***e***, anti-CD21 (10×); ***f***, anti-BCL2 (10×); ***g***, anti-BCL6 (10×); ***h***, anti-MYC (20×); and ***i***, anti-Ki-67 (20×).
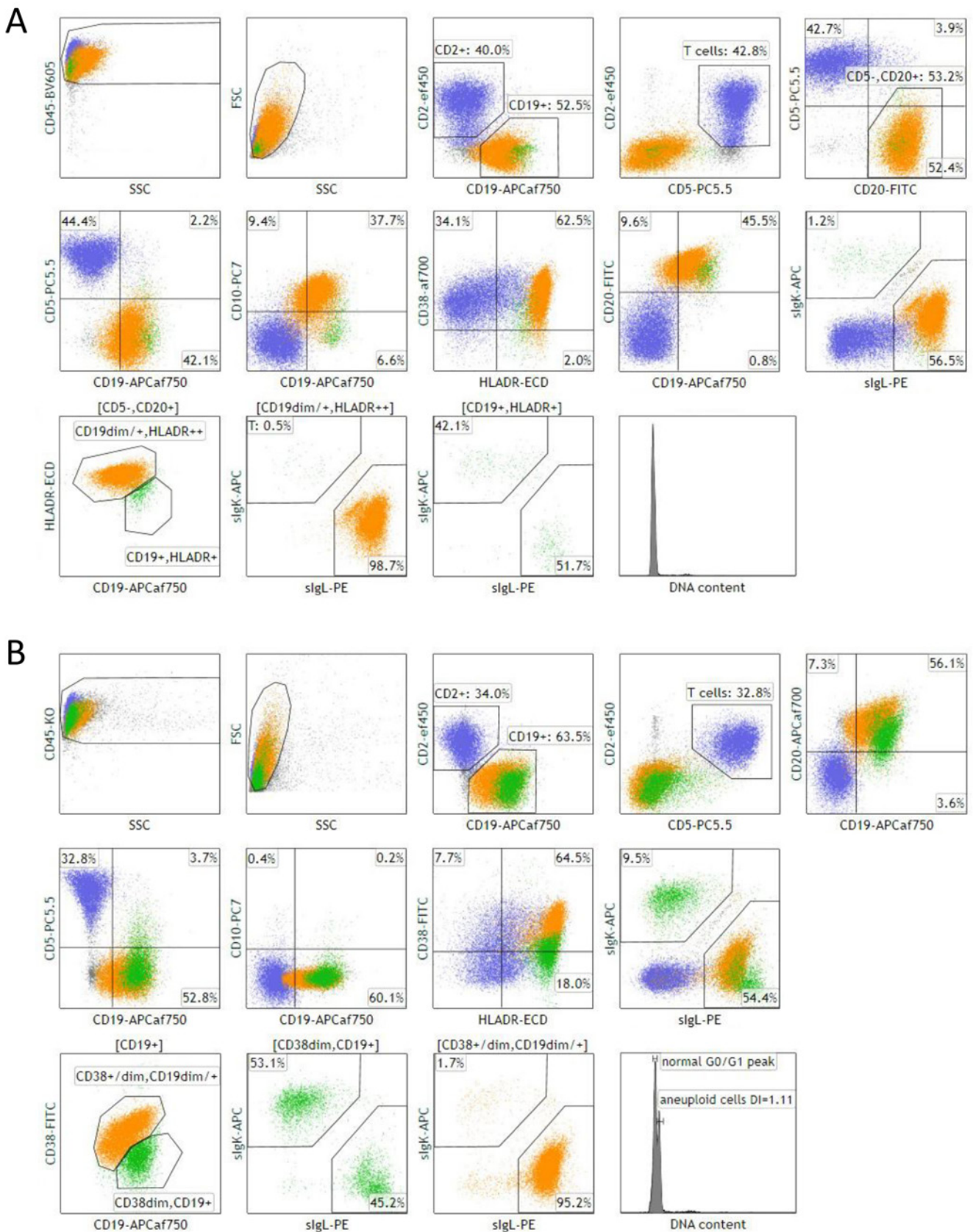
Fig. 2. Multicolor FCM of lymphoma cells in LN biopsies of case 1 (*A*) and case 2 (*B*) using fluorochrome-conjugated monoclonal antibodies. T cells (blue) were gated by the CD2/CD5 expression in both *A* and *B*. For B cells, the CD5⁻/CD20⁺ fraction was separated into the CD19dim/HLA-DR++ lymphoma cell (orange) and CD19+/HLA-DR+ polyclonal B-cell (green) populations in *A*, and the CD19+ fraction was separated into the CD38+/dim/CD19dim/+ lymphoma cell (orange) and CD38dim/CD19+ polyclonal B-cell (green) fractions in *B*. DNA indices were measured by independent FCM.
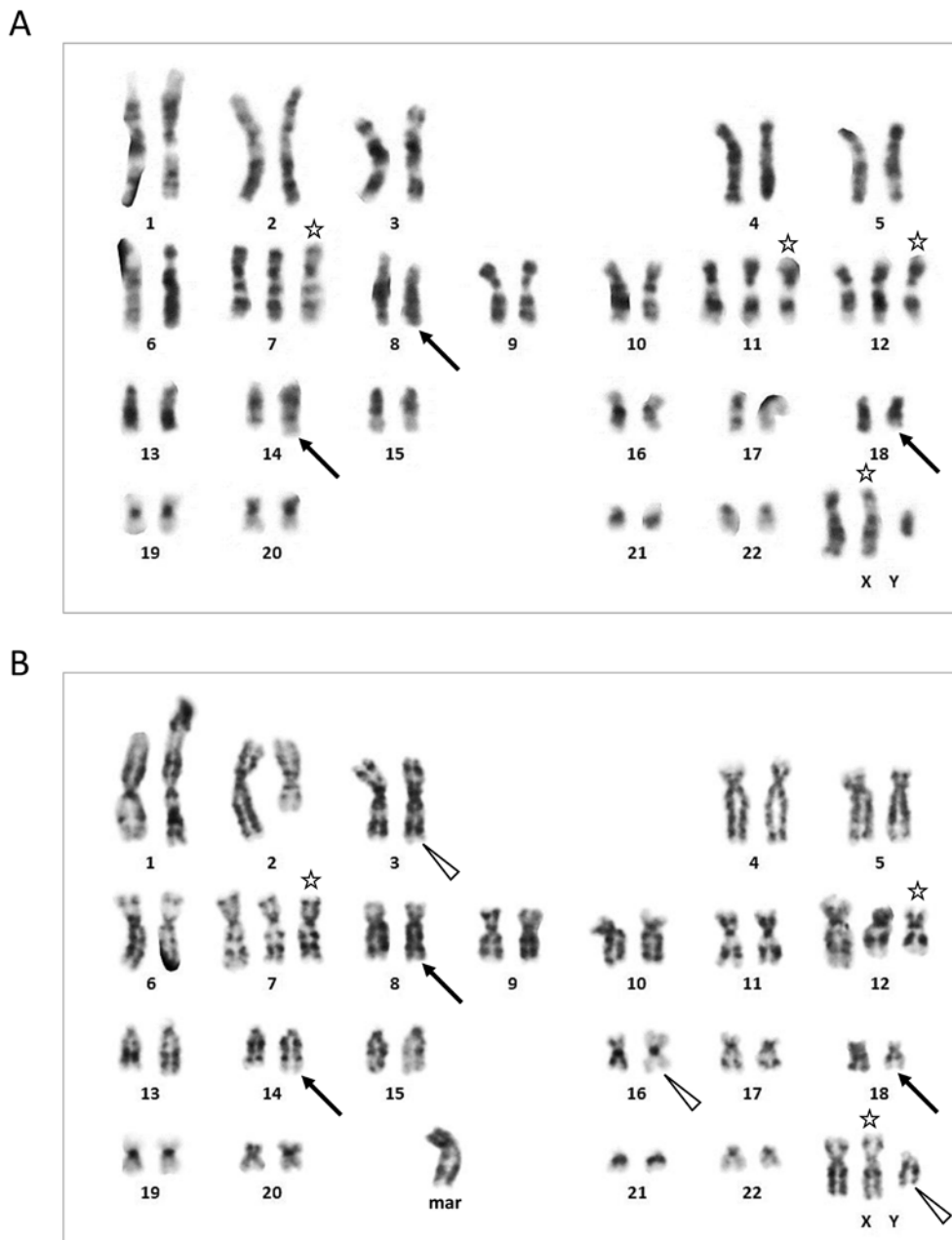
Fig. 3. G-banding karyotype of case 1 (*A*) and case 2 (*B*). t(8;14;18)(q24;q32;q21), indicated by the arrows, is recognized by lighter G-band of additional materials of der(14) than that created by t(14;18) (q32;q21) and darker and larger G-band of q24 of der(8), which actually represents the 18q22 band, than that of a normal chromosome 8 homolog. Numerical alterations are indicated by asterisks, and add(Y)(q12), der(3)t(3;16)(q27;p13), and ider(16)(p10) marker chromosomes in cases 2 are indicated by open arrowheads. The karyotypes are: 50,XY,+X,+7,t(8;14;18)(q24;q32;q21),+11,+12 in *A* and 50,XY,+X,add(Y)(q12),add(1)(p36),del(2)(q21),der(3)t(3;16)(q27;p13),+7,t(8;14;18) (q24;q32;q21),+del(12)(q24.1),ider(16)(p10)t(3;16)(q27;p13),+mar in *B*.

Ki-67–labeling index was higher in case 2 than in case 1. Nevertheless, both cases showed indolent clinical behavior and favorably responded to conventional chemotherapy approved for the treatment of FL.[18] Most importantly, both cases carried t(8;14;18), leading to *MYC*/*BCL2* DH. As hybridization of interphase nuclei carrying either t(8;14;18) or concurrent t(8;14)(q24;q32) and t(14;18)(q32;q21) with *MYC* or *BCL2* BA probes generates one red, one green, and one yellow signal, t(8;14;18) was only confirmed by FISH applied to the metaphase spreads. In case 2, as the result of t(3;16)(q27;p13), *BCL6* likely came under the control of the *CIITA* promotor activity

As the normal homolog of chromosome 14 was labeled by an unrearranged *IGH* FISH signal in both cases, *MYC* and *BCL2* were theoretically rearranged with the same *IGH* gene. Figure 6C represents the two-step translocation model involving the single *IGH* allele to create t(8;14;18) in case 1. The first translocation occurred between *BCL2*-MBR and

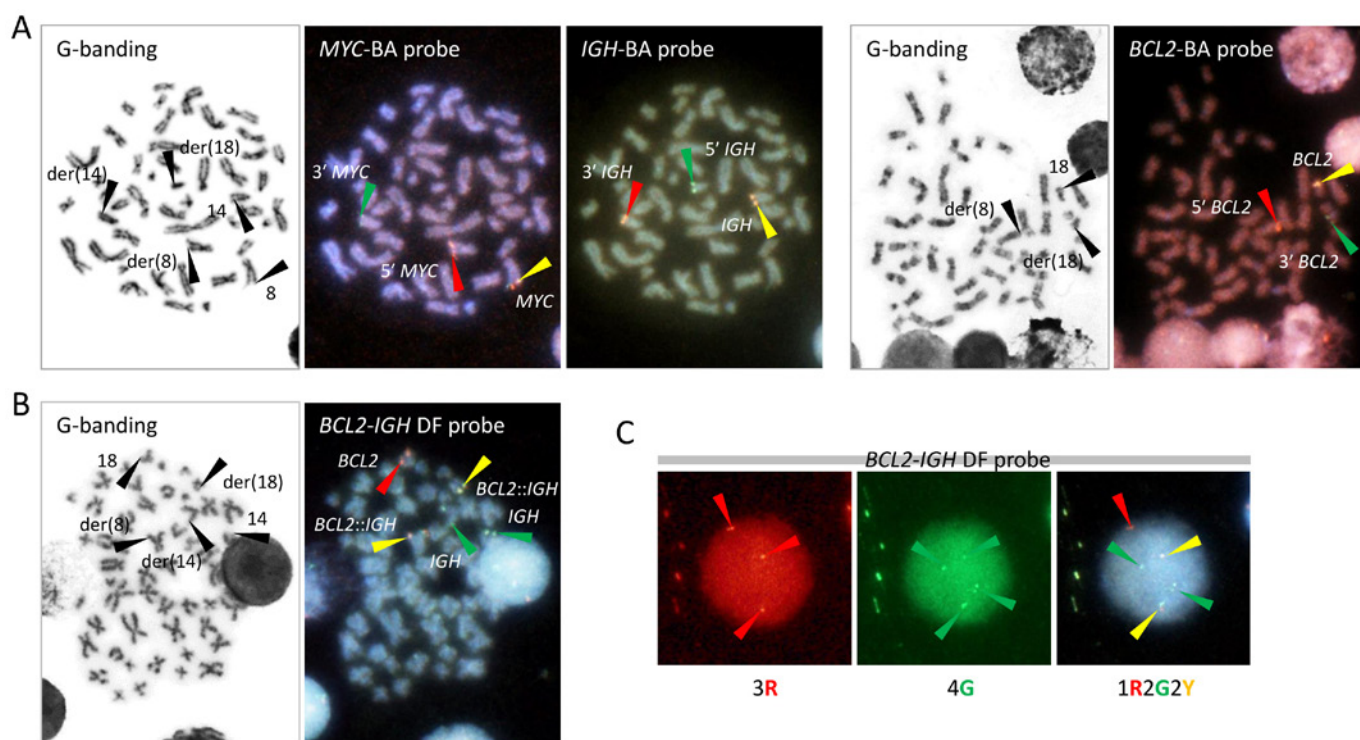**Fig. 4.** FISH of case 1. G-banding and FISH of metaphase spreads using *MYC*, *IGH*, and *BCL2* BA probes (***A***) and using the *BCL2-IGH* DF probe (***B***). Hybridization signals on the relevant chromosomes are indicated by the arrowheads of their respective colors. (***C***) FISH of interphase nuclei using the *BCL2-IGH* DF probe. Images through the TRITC, FITC, and triple band-pass filters are aligned. The one red (R), two green (G), and two yellow (Y) signal pattern is identical to and indistinguishable from those found in nuclei carrying t(14;18)(q32;q21)/*BCL2*::*IGH* and t(8;14)(q24;q32)/*MYC*::*IGH*. Diagrams of the FISH probes provided by the manufacturers are shown in Supplementary Figure S1.

IGHJ5, and the downstream constant gene was classswitched from *IGHM* to *IGHG1*. The second translocation occurred upstream of *MYC* exon 2 and within the switch region associated with *IGHA2*. As *IGHG1* is the secondmost upstream *IGHG* and *IGHA2* is the most downstream constant gene, this model can account for the development of *BCL2*::*IGH* and *MYC*::*IGH* that involved the same *IGH* allele. As the result of the second translocation, the 5′ *IGH* enhancer remains close to the *BCL2* coding exons, while the 3′ *IGH* enhancer leaves the *BCL2*::*IGH* fusion gene and comes close to the *MYC* coding exons. It remains to be determined whether the manner of *MYC* and *BCL2* activation resulting from t(8;14;18) is similar to or different from that of concurrent t(8;14) and t(14;18), in which *MYC* and *BCL2* are rearranged with the individual *IGH* allele.

t(8;14;18) was first described in a B-cell non-Hodgkin's lymphoma (B-NHL) cell line, DoHH2, and der(8) was found to comprise 5′ *MYC* (exon 1)-Sγ4-*JH6*-*BCL2* MBR.[19] Similar but more complex rearrangements were found in a transformed FL cell line, Tat-1, where the *BCL2*::*IGH*::*MYC* triple fusion element was duplicated and inserted within a site of der(13).[20] In a large series of British Columbia Cancer Agency, of a total of 1,350 cases of acute leukemia and malignant lymphoma, 8 had t(8;14;18) and/or exhibited FISH evidence for *MYC*::*IGH*::*BCL2* triple fusion on der(8).[21] Of these 8 cases, 3 initially presented with lymphoblastic lymphoma and 5 with FL grade 1, and all were finally diagnosed with HGBL not otherwise specified. Although it is unclear whether the cytogenetic study in each case was performed at presentation or transformation, the authors suggested the association of t(8;14;18) with HGBL histopathology.[21] In contrast, cases of FL associated with t(8;14;18) have been described in the literature.[22-24] One case reported from a Japanese institution presented with lymphadenopathy, hepatosplenomegaly, and leukemic manifestation.[24] Although the patient relapsed shortly after R-CHOP, FL grade 2 histopathology remained in the second biopsy. This and our current case reports suggest that the presence of t(8;14;18) in FL does not immediately indicate high-grade transformation and aggressive clinical behavior requiring intensive chemotherapy. Of course, however, early relapse and transformation to HGBL should be monitored carefully during and after treatment.

ACKNOWLEDGMENTS

CONFLICT OF INTEREST

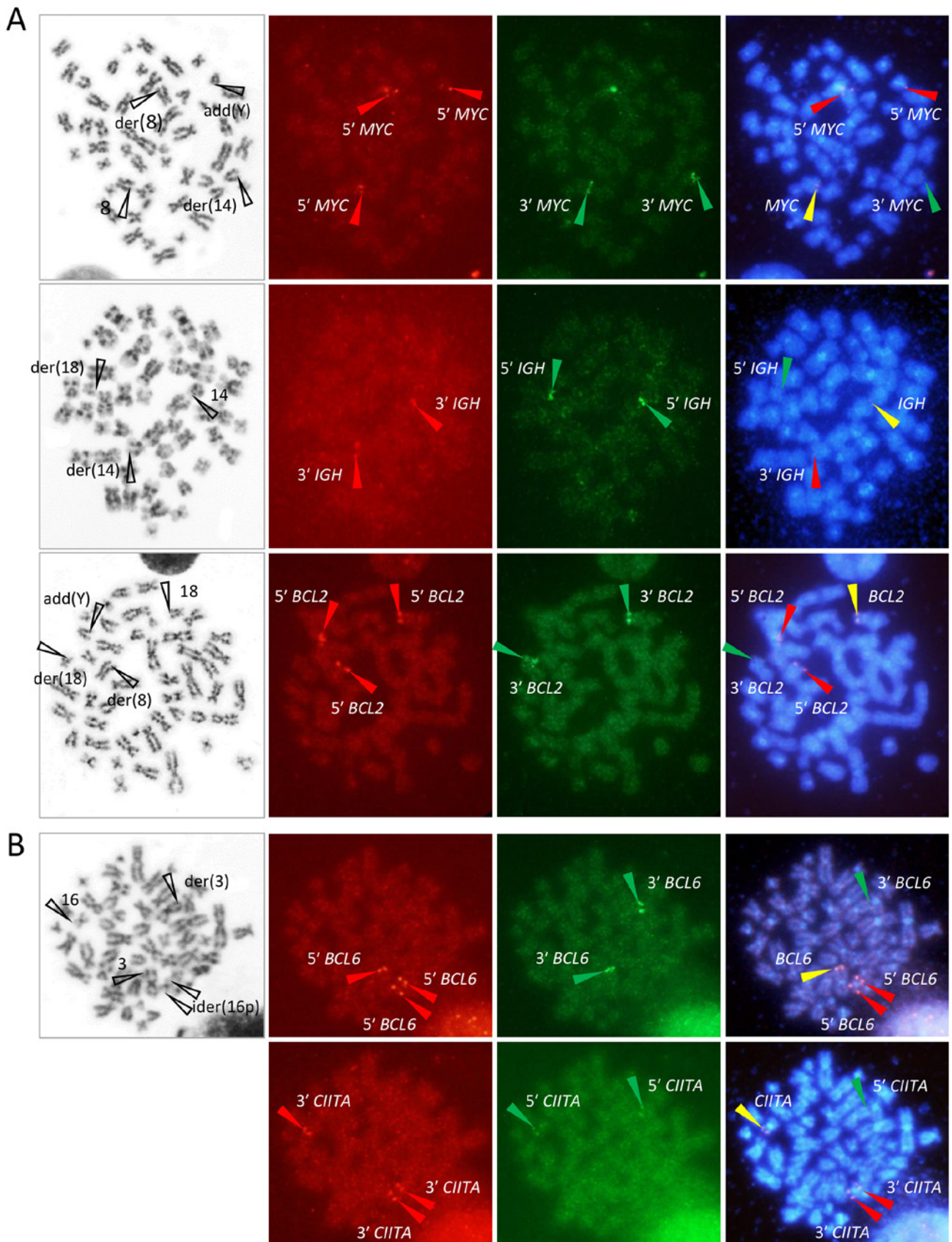The authors declare that they have no conflict of interest.

Fig. 5. FISH of case 2. (*A*) FISH of metaphase spreads using the *MYC* (*top*), *IGH* (*middle*), and *BCL2* (*bottom*) BA probes. (*B*) FISH of a metaphase spread using the *BCL6* (*top*) and *CIITA* (*bottom*) BA probes. G-banding and FISH through the TRITC, FITC, and triple band-pass filters are aligned. Hybridization signals on the relevant chromosomes are indicated by the arrowheads of their respective colors. Diagrams of the FISH probes provided by the manufacturers are shown in Supplementary Figure S1.
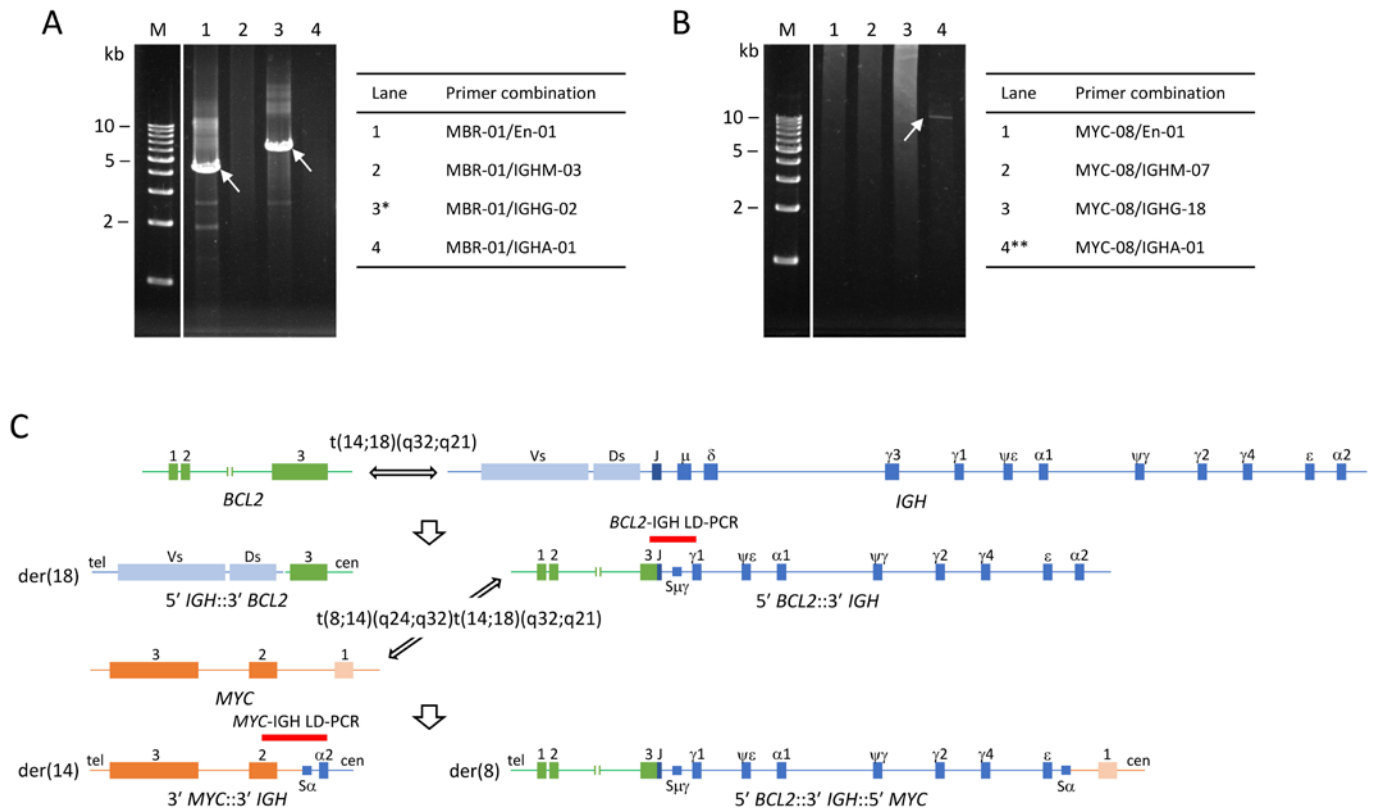
Fig. 6. Anatomy of t(8;14;18)(q24;q32;q21) in case 1. EtBr-stained gel electrophoresis of LD-PCR encompassing the t(14;18)(q32;q21)/*BCL2*::*IGH* (**A**) and t(8;14)(q24;q32)/*MYC*::*IGH* (**B**) junctions.[16] Nucleotide sequencing of the LD-PCR products generated by the *MBR-01/IGHG-02 and **MYC-08/IGHA-01 primer combinations confirmed *BCL2*-MBR:*IGHJ5*::*IGHG1* and *MYC* exon 2::*IGHA2* fusions. The sequences of the primers used in this study are listed in Supplementary Table S1. (**C**) Schematic diagram of the two-step translocation to generate t(8;14;18), involving *MYC* (8q24), *IGH* (14q32), and *BCL2* (18q21). According to this model, this translocation is more precisely described as: der(8)t(8;14)(q24;q32)t(14;18)(q32;q21),der(14)t(8;14)(q24;q32),der(18)t(14;18)(q32;q21). The 3′ *IGH* segment on the der(8) chromosome is labeled by the *IGH* probe of the *BCL2-IGH* DF probe, but is not covered by the *IGH* BA probe. cen, centromere; tel, telomere.

REFERENCES

1 Kluin PM, Harris NL, Stein H, *et al.* High-grade B-cell lymphoma. In: Swerdlow SH, Campo E, Harris NL, *et al.* (eds): WHO Classification of Tumours of Haematopoietic and Lymphoid Tissues. 4th ed, Lyon, IARC. 2017; pp. 335-341.

2 Alaggio R, Amador C, Anagnostopoulos I, *et al.* The 5th edition of the World Health Organization Classification of Haematolymphoid Tumours: Lymphoid Neoplasms. Leukemia. 2022; 36: 1720-1748.

3 Campo E, Jaffe ES, Cook JR, *et al.* The International Consensus Classification of Mature Lymphoid Neoplasms: a report from the Clinical Advisory Committee. Blood. 2022; 140: 1229-1253.

4 Aukema SM, Siebert R, Schuuring E, *et al.* Double-hit B-cell lymphomas. Blood. 2011; 117: 2319-2331.

5 Friedberg JW. How I treat double-hit lymphoma. Blood. 2017; 130: 590-596.

6 Chihara D, Ito H, Matsuda T, *et al.* Differences in incidence and trends of haematological malignancies in Japan and the United States. Br J Haematol. 2014; 164: 536-545.

7 Jaffe ES, Harris NL, Swerdlow SH, *et al.* Follicular lymphoma. In: Swerdlow SH, Campo E, Harris NL, et al. (eds): WHO Classification of Tumours of Haematopoietic and Lymphoid Tissues. 4th ed, Lyon, IARC. 2017; pp. 266-273.

8 Muramatsu M, Akasaka T, Kadowaki N, *et al.* Rearrangement of the *BCL6* gene in B-cell lymphoid neoplasms: comparison with lymphomas associated with *BCL2* rearrangement. Br J Haematol. 1996; 93: 911-920.

9 Höglund M, Sehn L, Connors JM, *et al.* Identification of cytogenetic subgroups and karyotypic pathways of clonal evolution in follicular lymphomas. Genes Chromosomes Cancer. 2004; 39: 195-204.

10 Ikoma H, Miyaoka M, Hiraiwa S, *et al.* Clinicopathological analysis of follicular lymphoma with BCL2, BCL6, and MYC rearrangements. Pathol Int. 2022; 72: 321-331.

11 Miao Y, Hu S, Lu X, *et al.* Double-hit follicular lymphoma with *MYC* and *BCL2* translocations: a study of 7 cases with a review of literature. Hum Pathol. 2016; 58: 72-77.

12 Miyaoka M, Kikuti YY, Carreras J, *et al.* Clinicopathological and genomic analysis of double-hit follicular lymphoma: comparison with high-grade B-cell lymphoma with *MYC* and *BCL2* and/or *BCL6* rearrangements. Mod Pathol. 2018; 31: 313-326.

13 Chaudhary S, Brown N, Song JY, *et al.* Relative frequency and clinicopathologic characteristics of *MYC*-rearranged follicular lymphoma. Hum Pathol. 2021; 114: 19-27.

14 Ziemba JB, Wolf Z, Weinstock M, Asakrah S. Double-hit and triple-hit follicular lymphoma. Am J Clin Pathol. 2020; 153:

672-685.

15 McGowan-Jordan J, Hastings RJ, Moore S, eds. ISCN 2020: An International System for Human Cytogenomic Nomenclature. Basel, S. Karger AG. 2020.

16 Akasaka T, Akasaka H, Ohno H. Polymerase chain reaction amplification of long DNA targets: application to analysis of chromosomal translocations in human B-cell tumors (review). Int J Oncol. 1998; 12: 113-121.

17 Akasaka H, Akasaka T, Kurata M, *et al.* Molecular anatomy of *BCL6* translocations revealed by long-distance polymerase chain reaction-based assays. Cancer Res. 2000; 60: 2335-2341.

18 Marcus R, Davies A, Ando K, *et al.* Obinutuzumab for the first-line treatment of follicular lymphoma. N Engl J Med. 2017; 377: 1331-1344.

19 Dyer MJ, Lillington DM, Bastard C, *et al.* Concurrent activation of *MYC* and *BCL2* in B cell non-Hodgkin lymphoma cell lines by translocation of both oncogenes to the same immunoglobulin heavy chain locus. Leukemia. 1996; 10: 1198-1208.

20 Denyssevych T, Lestou VS, Knesevich S, *et al.* Establishment and comprehensive analysis of a new human transformed follicular lymphoma B cell line, Tat-1. Leukemia. 2002; 16: 276-283.

21 Knezevich S, Ludkovski O, Salski C, *et al.* Concurrent translocation of *BCL2* and *MYC* with a single immunoglobulin locus in high-grade B-cell lymphomas. Leukemia. 2005; 19: 659-663.

22 Tilly H, Rossi A, Stamatoullas A, *et al.* Prognostic value of chromosomal abnormalities in follicular lymphoma. Blood. 1994; 84: 1043-1049.

23 Le Baccon P, Leroux D, Dascalescu C, *et al.* Novel evidence of a role for chromosome 1 pericentric heterochromatin in the pathogenesis of B-cell lymphoma and multiple myeloma. Genes Chromosomes Cancer. 2001; 32: 250-264.

24 Minakata D, Sato K, Ikeda T, *et al.* A leukemic double-hit follicular lymphoma associated with a complex variant translocation, t(8;14;18)(q24;q32;q21), involving BCL2, MYC, and IGH. Cancer Genet. 2018; 220: 44-48.